Model Predictive Control Based Ramp Minimization in Active Distribution Network Using Energy Storage Systems

Jiayong Li[1], Zhao Xu[1], Jian Zhao[1,2], Songjian Chai[1], Yi Yu[3], Xu Xu[1]

[1]*Department of Electrical Engineering, The Hong Kong Polytechnic University, Hong Kong, P. R. China, Email: j-y.li@connect.polyu.hk, eezhaoxu@polyu.edu.hk, zhaojianee@foxmail.com, steven.chai@connect.polyu.hk, benxu.xx@connect.polyu.hk*

[2]*Department of Electrical Power Engineering, Shanghai University of Electric Power, Shanghai, China, Email: zhaojianee@foxmail.com*

[3]*Schoole of Electrical Engineering, Wuhan University, Wuhan, China, Email: yuyiyuyi@whu.edu.cn*

Model Predictive Control Based Ramp Minimization in Active Distribution Network Using Energy Storage Systems

Jiayong Li[1], Zhao Xu[1], Jian Zhao[1,2], Songjian Chai[1], Yi Yu[3], Xu Xu[1]

[1]*Department of Electrical Engineering, The Hong Kong Polytechnic University, Hong Kong SAR, China. Email: j-y.li@connect.polyu.hk, eezhaoxu@polyu.edu.hk, zhaojianee@foxmail.com, steven.chai@connect.polyu.hk, benxu.xx@connect.polyu.hk*

[2]*Department of Electrical Power Engineering, Shanghai University of Electric Power, Shanghai, China, Email: zhaojianee@foxmail.com*

[3]*Schoole of Electrical Engineering, Wuhan University, Wuhan, China. Email: yuyiyuyi@whu.edu.cn*

Abstract- The growing integration of renewable energy sources, especially the residential photovoltaic (PV) systems, in the distribution networks (DNs) aggravates the ramp-events in transmission system. In order to address this issue, we propose a novel look ahead dispatch model for the ramp minimization in DNs using distributed energy storage systems (ESSs). The dispatch problem considering the scheduling of ESSs is modelled as a finite-horizon optimization problem and is carried out using model predictive control (MPC) method that takes both current and future information into account. In addition, the optimal power flow in DN is formulated as a second-order cone programming problem to guarantee the global optimality. Numerical results on IEEE 37-bus distribution network show that our proposed model not only brings about 74% reduction of maximum ramp but also yields the near-minimum system operating cost.

Keywords: Active distribution network, ramp-event, energy storage system, model predictive control.

1 Introduction

The distribution networks (DNs) are undergoing a transition from traditional passive networks to active networks due to the growing integration of distributed energy resources (DERs), the infusion of smart meters as well as the emergence of advanced information and communication technologies (ICT) [1]. The evolution of the distribution networks constitutes an important aspect of the smart grid and has the following advantages. Firstly, the sustainability and reliability of power supply can be improved since a large proportion of DERs are renewable energy based and can meet the demand of local customers. Secondly, the operational flexibility and efficiency can also be enhanced due to the capability of reliable real-time monitoring, effective real-time communication and advanced real-time control in active DNs [2]. Thirdly, active DNs also enables implementation of efficient and competitive market designs, such as peer-to-peer energy transaction and demand response, by leveraging the advantage of smart meters and ICTs. In order to fully unlock the economic and technical value of active DNs, a non-profit distribution System Operator (DSO) is required to operate the DN securely, reliably and efficiently like an Independent System Operator (ISO) in transmission network [3]. Even though the transition of DNs produces various benefits, it also causes troubles to the system operation and control especially when the penetration of renewable distributed generators (DGs), e.g. distributed wind turbines and rooftop PV installations, is high. One of the biggest challenges arises from the scarcity of flexible ramping products to tackle the significant variation of net load and thus resulting in the reduction of operational reliability [4]. Since the ramping effect in the DNs will be translated into the transmission network and aggravate the shortage of ramping capability, it is necessary for DSOs to address the

ramping problem locally with local flexible resources, e.g. energy storage systems.

Net load, defined as the difference between the actual load and the renewable generation, has been widely used to investigate the impact of renewable energy sources (RESs) integration. Over the years, the California Independent System Operator (CAISO) has observed a sharp decline during the sunrise and a steep rise during the sunset of the daily net load curve, which is known as the "duck curve" [5]. As a result, the duck curve of net load imposes a hard ramp-down and ramp-up requirement on power systems. In order to address this issue, several approaches have been proposed. For instance, ref. [6] proposes a ramp limitation oriented control strategy for large scale PV power plants considering the PV curtailment. Though it is effective in controlling the PV ramp, it also leads to the reduction of economic and environmental benefit of RES. Another method is to design new products called flexible ramping products (FRPs) and procure them from the market, which has been extensively studied before recent implementation by CAISO and Midcontinent ISO (MISO) [7]. Ref. [4] evaluates the influence of FRPs on the optimal economic dispatch and shows that FRPs can reduce dispatch cost. Ref. [8] presents a comprehensive review on the modelling and utilization of FRPs. To sum up, much effort has been made to alleviate the ramping effect in transmission networks. Nevertheless, few works have studied the ramping problem in DNs even though it can aggravate the shortage of ramping capacity in transmission networks.

Energy storage system (ESS) is believed to be an effective option to accommodate the high penetration of RES. It has gained overwhelming popularity around the world because of its considerable benefits [9], e.g. deferring the upgrade of generation and network, reducing operating cost and RES curtailment, enhancing system operational

flexibility, achieving low-carbon objective, etc. ESS can be classified into utility-scale ESS installed in transmission system and distributed ESS located in DNs and microgrids (MGs). Both types of ESS can provide various services to the power system. In [10], the large-scale ESSs are employed to relieve transmission congestion. In [11], ESSs are scheduled to fulfil the peak-shaving and valley-filling of the netload in distribution system. In [12], ESSs are utilized to minimize the total operating cost of the distribution network. In [13], ESSs play an important role in providing flexible ramping products to transmission network. In [14], ESSs are utilized to enhance the system security by taking corrective action after a contingency. In this paper, we endeavour to minimize ramping effect in DNs using distributed ESSs.

To deal with the uncertainties of load demand and renewable energy output, several methods have been proposed, e.g. stochastic programming [15], robust optimization [16] and model predictive control (MPC) [17]. However, MPC is recognized to be more suitable for short-term operation problem due to its underlying rolling optimization manner. Thus, we will use MPC to carry out our proposed ramp minimization dispatch model. Up to now, MPC has been widely applied in power systems, such as appliance scheduling of a residential building [17], energy management of isolated microgrids [18], real-time power system protection [19].

In active DNs, the power flow is no longer unidirectional from the substation to the end-use customers. In order to effectively model bidirectional power flow in active DNs, Baran and Wu proposed a branch flow model in [20], [21]. However, the original branch flow model is nonconvex, which poses challenge in finding a global optimal solution. In this regard, a convexified branch flow model was derived by Farivar and Low in [22] based

on the second-order cone relaxation and has been widely used since then. To guarantee the global optimality, the second-order cone relaxed branch flow model is also used in our proposed ramp minimization problem.

This paper proposes a novel MPC based dispatch model for ramp minimization in active DNs using distributed ESSs. The main contributions are summarized as follows.

- We propose a novel look ahead dispatch model for the ramp minimization in active DNs. The fast responding ESSs are employed to offset the ramp-up and ramp-down event caused by the distributed PV generations. To the best of our knowledge, few works have studied the ramping problem in distribution systems.
- Model predictive control method is used to carry out our proposed dispatch model, which incorporates both current information and newly updated forecast information. Consequently, ESSs can be appropriately scheduled to avoid latent over-charging or over-discharging during some periods. Moreover, we employ the second-order cone relaxed branch flow model to formulate the power flow in active DNs so as to guarantee the global optimality.
- Numerical results demonstrate that our proposed MPC based ramp minimization model not only brings about significant reduction of ramping effect (74% reduction of maximum ramp), but also yields economically efficient result.

The rest of paper is organized as follows. Section 2 presents the system model and the problem formulation of the proposed ramp minimization problem in active DNs. Section 3 applies the MPC approach to the ramp minimization problem. In section 4, we demonstrate the numerical results. Finally, section 5 concludes the paper.

2 System Model and Problem Formulation

2.1 Branch Flow Model in Distribution Networks

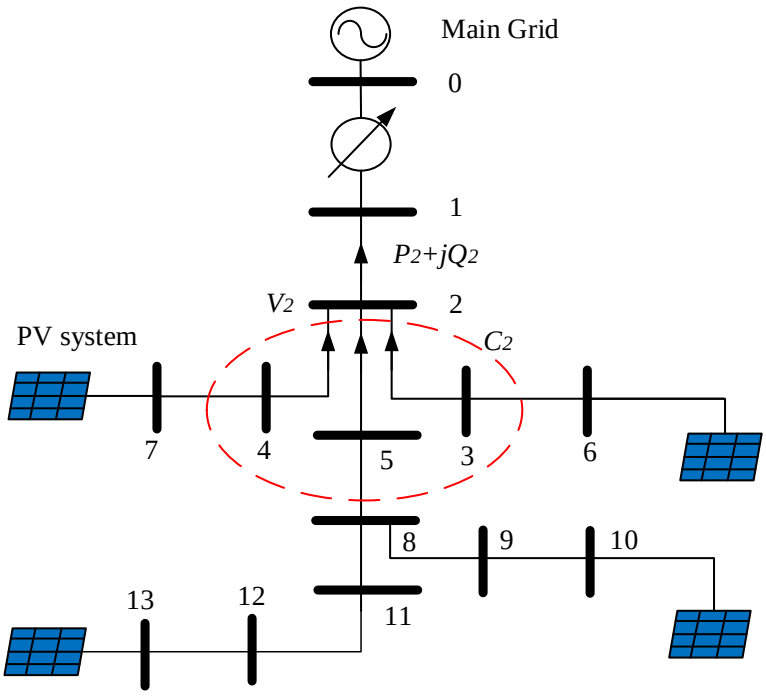

Fig. 1. A typical radial distribution network

Consider a distribution network (DN), which is typically radial as shown in Fig. 1. Let $\mathcal{G} := (\mathcal{N}, \mathcal{E})$ denote the topology of the DN, where $\mathcal{N} := \{0,1,\ldots,N\}$ represents the set of buses and $\mathcal{E}$ represents the set of directed lines. Note that each bus i except the substation bus (indexed by 0) has a unique ancestor bus, denoted by A_i, and a set of child buses, denoted by C_i. For instance, bus 2 has a unique ancestor which is bus 1 and several child buses including bus 3, 4 and 5, i.e. $A_2 = 1$ and $C_2 = \{3,4,5\}$. Moreover, the direction of each line is assumed from a bus i to its ancestor bus A_i as illustrated in Fig. 1. Thus, we uniquely label the line from bus i to its ancestor bus A_i as i so that the label of line is consistent with label of the bus and we have $\mathcal{E} := \{1,\ldots,N\}$. In a radial distribution network, branch flow model (BFM) has been widely used to model the power flow equations [22].

Specifically, the active power balance at the substation bus and other buses can be represented by Eq. (1) and (2), respectively.

$$\sum_{j\in C_0}(P_{j,\tau}-r_j l_{j,\tau})+p_{0,\tau}=0 \tag{1}$$

$$\sum_{j\in C_i}(P_{j,\tau}-r_j l_{j,\tau})+p_{i,\tau}=P_{i,\tau} \qquad \forall i\in\mathcal{N}\setminus 0 \tag{2}$$

where $p_{0,\tau}$ and $p_{i,\tau}$ denote the active power injection (+) or extraction (-) at the substation bus and other bus i at time τ, respectively; $P_{j,\tau}$ and $l_{j,\tau}$ represent the active power flow and squared line current magnitude on line j at time τ, respectively; r_j is the resistance of line j.

The reactive power balance at the substation bus and other buses is represented by Eq. (3) and (4), respectively.

$$\sum_{j\in C_0}(Q_{j,\tau}-x_j l_{j,\tau})+q_{0,\tau}=0 \tag{3}$$

$$\sum_{j\in C_i}(Q_{j,\tau}-x_j l_{j,\tau})+q_{i,\tau}=Q_{i,\tau} \qquad \forall i\in\mathcal{N}\setminus 0 \tag{4}$$

where $q_{0,\tau}$ and $q_{i,\tau}$ denote the reactive power injection (+) or extraction (-) at the substation bus and other bus i at time τ, respectively; $Q_{j,\tau}$ is the reactive power flow on line j at time τ. x_j is the reactance of line j.

The voltage drop/rise on each line can be described by Eq. (5).

$$v_{i,\tau}-v_{A_i,\tau}=2(r_i P_{i,\tau}+x_i Q_{i,\tau})-(r_i^2+x_i^2)l_{i,\tau} \qquad \forall i\in\mathcal{E} \tag{5}$$

where $v_{i,\tau}$ is the squared bus voltage magnitude of bus i at time τ.

The relationship between the power flow, squared bus voltage magnitude and squared line current magnitude can be expressed by Eq. (6).

$$l_{i,\tau} = \frac{P_{i,\tau}^2 + Q_{i,\tau}^2}{v_{i,\tau}} \qquad \forall i \in \mathcal{E} \tag{6}$$

Note that Eq. (6) is nonconvex, which makes it computational challenging to find the global optimal solution to the OPF problem. In order to convexify Eq. (6), it is relaxed into an inequality as Eq. (7) and then reformulated into a second-order cone constraint as Eq. (8).

$$l_i \geq \frac{P_i^2 + Q_i^2}{v_i} \qquad \forall i \in \mathcal{E} \tag{7}$$

$$\left\| (2P_i,\ 2Q_i,\ l_i - v_i) \right\|_2 \leq l_i + v_i \qquad \forall i \in \mathcal{E} \tag{8}$$

It has been proved in [22] that the relaxation is exact as long as the network is radial and the objective function of the OPF problem is strictly increasing in l_i. In our model, the equality in (7) also holds since we take the network loss into account and it is a strict increasing function of l_i.

In an OPF problem, the voltage magnitude of each bus and current magnitude of each line should be maintained within the acceptable ranges.

$$(V_i^{\min})^2 \leq v_{i,\tau} \leq (V_i^{\max})^2 \qquad \forall i \in \mathcal{N} \tag{9}$$

$$l_{i,\tau} \leq (I_i^{\max})^2 \qquad \forall i \in \mathcal{E} \tag{10}$$

where $V_i^{\min}$ and $V_i^{\max}$ denote the upper and lower bounds of voltage magnitude at bus *i*, $I_i^{\max}$ is the line current capacity of line *i*.

2.2 Ramp events and Ramp Index

Fig. 2 shows a typical net load curve with high penetration of PV generation. Severe ramp-down and ramp-up events are indicted in the figure, which are caused by the diurnal

generation pattern of PV systems. Consequently, more and more ramping products are needed, which will eventually lead to the shortage of ramping capability. Therefore, we particularly focus on mitigating the ramping effect in distribution systems so as to alleviate the shortage of ramping capability in transmission grid. To this end, we first define the ramp index in DNs for each time slot t to quantify the ramping effect, as shown below.

$$IR_t = \left| p_{0,t} - p_{0,t-1} \right| \tag{11}$$

where $p_{0,t}$ is the power injection/extraction of the distribution network to/from the main grid at time slot t. Thus, it also represents the total net load of the entire distribution network.

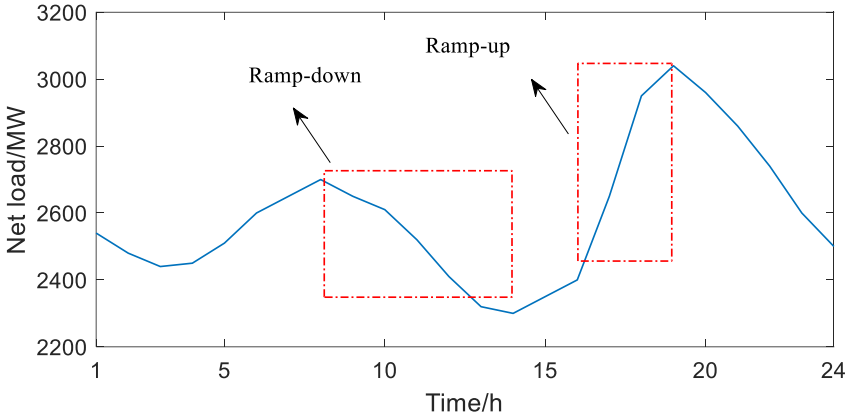

Fig. 2. A typical daily net load curve with the illustration of ramp events

2.3 Energy Storage System Model

Over the past few years, great advances have been made in the battery storage technologies, especially in the lithium-ion battery. In this paper, the battery ESSs are utilized to mitigate the ramping effect through charging during the ramp-down events of the net load and discharging during the ramp-up event of the net load. Since the detailed battery ESS technologies are beyond the scope of this paper, we will only present the generic mathematical model of ESSs. Let $p_{k,\tau}^{char}$ and $p_{k,\tau}^{disc}$ denote the charging and

discharging power of *k*-th ESS at time slot τ. The charging and discharging power at each time slot should be maintained within the allowable ranges, as shown below.

$$0 \le p_{k,\tau}^{char} \le \overline{p}_k^{char} \quad \forall k \in \mathcal{N}^{ess} \tag{12}$$

$$0 \le p_{k,\tau}^{disc} \le \overline{p}_k^{disc} \quad \forall k \in \mathcal{N}^{ess} \tag{13}$$

where $\overline{p}_k^{char}$ and $\overline{p}_k^{disc}$ are the upper bound of charging and discharging power of *k*-th ESS, respectively; $\mathcal{N}^{ess}$ denotes the set of ESS.

The dynamics of ESSs between two successive time slots can be described as

$$S_{k,\tau} = S_{k,\tau-1} + (\eta_k^{char} \cdot p_{k,\tau}^{char} - 1/\eta_k^{disc} \cdot p_{k,\tau}^{disc}) \cdot \Delta t \quad \forall k \in \mathcal{N}^{ess} \tag{14}$$

where $S_{k,\tau}$ is the state of charge (SOC) of *k*-th ESS at the end of time slot τ; η_k^{char} and η_k^{disc} denote the charging efficiency and discharging efficiency, respectively; Δt is the duration of one time slot.

The SOC should not exceed the maximum allowed level $S_k^{\max}$ or fall below the minimum allowed level $S_k^{\min}$, as shown below.

$$S_k^{\min} \le S_{k,\tau} \le S_k^{\max} \quad \forall k \in \mathcal{N}^{ess} \tag{15}$$

Frequent employment of ESS will shorten its life span. Thus, the degradation cost should be considered to avoid overuse of ESS. In our model, the degradation cost is modeled as a linear function of charging and discharging power like [23].

$$C_{k,\tau}^{d} = c_k^{d} \cdot (\eta_k^{char} p_{k,\tau}^{char} + p_{k,\tau}^{disc} / \eta_k^{disc}) \cdot \Delta t \tag{16}$$

where $C_{k,\tau}^{d}$ is degradation cost of *k*-th ESS at time slot τ and c_k^{d} denotes the unit degradation cost.

2.4 Multi-period Dispatch Model for Ramp Minimization

In this subsection, we propose a multi-period dispatch model for the distribution system operator (DSO) to mitigate the ramping effect and meanwhile to ensure the system operation is under a normal condition by leveraging the full potential of ESSs in providing ramping support. The objective not only considers the ramp index, but also takes network loss and ESS degradation cost into consideration. Since the units of the three items are not unified, we multiply the ramp index and network loss by the ramping price c_τ^r and electricity price c_τ^e, respectively, to present these two items in the monetary unit as well. In order to maintain the bus voltage magnitudes within the acceptable ranges, static voltage compensators (SVCs) are considered to provide voltage regulation support to the distribution system. The objective of the proposed model is to minimize the total cost composed of ramping cost, the cost of network loss and ESS degradation cost, and the constraints include the branch flow model, ESS model and SVC model. The detailed problem formulation is given as follows.

$$\min \sum_{t}^{t+M}\left(c_\tau^r \cdot \left| p_{0,\tau} - p_{0,\tau-1} \right| + c_\tau^e \sum_{i\in\mathcal{E}} r_i l_{i,\tau} + \sum_{k\in\mathcal{N}^{ess}} C_{k,\tau}^d \right) \tag{17a}$$

variables: $p_{0,\tau}, q_{0,\tau}, p_{k,\tau}^{disc}, p_{k,\tau}^{char}, S_{k,\tau}, q_{w,\tau,}^{svc}, P_{j,\tau}, Q_{j,\tau}, l_{j,\tau}, v_{i,\tau}$

s.t. (1)-(5), (8)-(10) $\quad \tau = t,...,t+M$ (17b)

$$p_{i,\tau} = \sum_{g\in\mathcal{N}^{pv}} b_{ig}^{pv} p_{g,\tau}^{pv} + \sum_{k\in\mathcal{N}^{ess}} (b_{ik}^{ess} p_{k,\tau}^{disc} - b_{ik}^{ess} p_{k,\tau}^{char}) - p_{i,\tau}^{l} \quad \forall\, i \in \mathcal{N}\setminus 0,\ \tau = t,...,t+M \tag{17c}$$

$$q_{i,\tau} = \sum_{w\in\mathcal{N}^{svc}} b_{iw}^{svc} q_{w,\tau}^{svc} - q_{i,\tau}^{l} \qquad \forall i \in \mathcal{N}\setminus 0,\ \tau = t,...,t+M \tag{17d}$$

$$v_{0,\tau} = 1 \qquad \tau = t,...,t+M \tag{17e}$$

$$(12)\text{-}(15) \qquad \tau = t,...,t+M \tag{17f}$$

$$\underline{q}_w \le q^{svc}_{w,\tau} \le \bar{q}_w \qquad \forall w \in \mathcal{N}^{svc},\ \tau = t,...,t+M \tag{17g}$$

where the first, second and third terms in (17a) represent the ramping cost, the cost of network loss and total degradation cost at time τ, respectively. Eq. (17b) describes the branch flow model. Eq. (17c) shows the active power injection at bus *i*, where $p^{pv}_{g,\tau}$, $p^{char}_{k,\tau}$ and $p^{disc}_{k,\tau}$ denote the *g*-th PV output, charging and discharging power of *k*-th ESS, respectively, $p^{l}_{i,\tau}$ is the active load of bus *i*, b^{pv}_{ig} and b^{ess}_{ik} are known binary indicators. $b^{pv}_{ig}=1$ if *g*-th PV system is located at bus *i*, and $b^{pv}_{ig}=0$ otherwise. Similarly, $b^{ess}_{ik}=1$ if *k*-th ESS is located at bus *i*, and $b^{ess}_{ik}=0$ otherwise. Eq. (17d) shows the reactive power injection at bus *i*, where $q^{svc}_{w,\tau}$ denotes the reactive power output of *w*-th SVC, $q^{l}_{i,\tau}$ denotes the reactive load of bus *i*, b^{svc}_{iw} is a known binary indicator. $b^{svc}_{iw}=1$ if *w*-th SVC is located at bus *i*, and $b^{svc}_{iw}=0$ otherwise. Eq. (17e) shows the voltage magnitude at the substation bus. Eq. (17f) describes the ESS model and Eq. (17g) imposes the limits on the SVC output.

3 Model Predictive Control based Implementation

The MPC method is employed to carry out our proposed dispatch model for ramp minimization. The key idea of MPC is to solve a finite horizon optimization problem in a receding horizon manner based on the latest updated information, but each time only the optimization result of the current time slot will be applied, as illustrated by Fig. 3. We assume at any time slot *t*, only the current load and PV information is accurate and known to the DSO. The future information of the load demand and PV generation is uncertain. Thus, the DSO needs to predict the load demand and PV generation for the following *M*-1 time slots using advanced forecast techniques as those in [24], [25]. Since the methodology

of load and PV forecasting is beyond the scope of this paper, we will not present it in this paper. The detailed procedure to implement the MPC based dispatch model is illustrated as below.

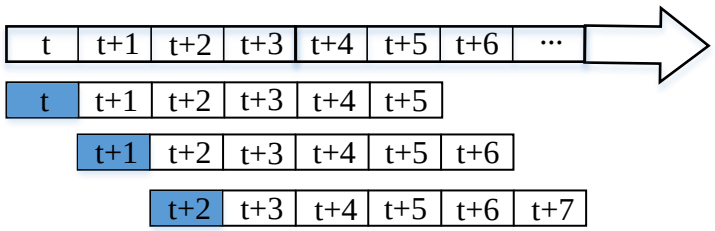

Fig. 3. Illustration of model predictive control with a horizon of 6 time slots

i) At time slot *t*, the DSO collects the load and PV information of the current time slot and updates their forecast information for the following *M*-1 time slots.

ii) Based on the information obtained at step i), the DSO solves the multi-period dispatch problem for the ramp minimization and only applies the optimal solution of the current time slot *t* to the ESSs and SVCs.

iii) When the time moves forward to *t*+1, the DSO executes exactly the same procedure described at step i) and ii).

Since the MPC method takes both current and future information into account, the short-sightedness in ESS scheduling can be avoided. Moreover, owing to the rolling optimization manner of the MPC method, the distributed system operator is enabled to correct its decision at each time slot based on the newly updated information. Hence, the impact of the load and PV forecast inaccuracy is substantially lessened. Note that increasing the horizon length may produce a more robust result, but it also leads to the decline of forecast accuracy and increase of optimization complexity. Thus, there is trade-off in selecting the length of the horizon. In our application, we consider a horizon of 6 time slots with the duration of each time slot being 1h. Fig. 4 shows the flowchart for the

implementation of the proposed MPC based ramp minimization dispatch model.

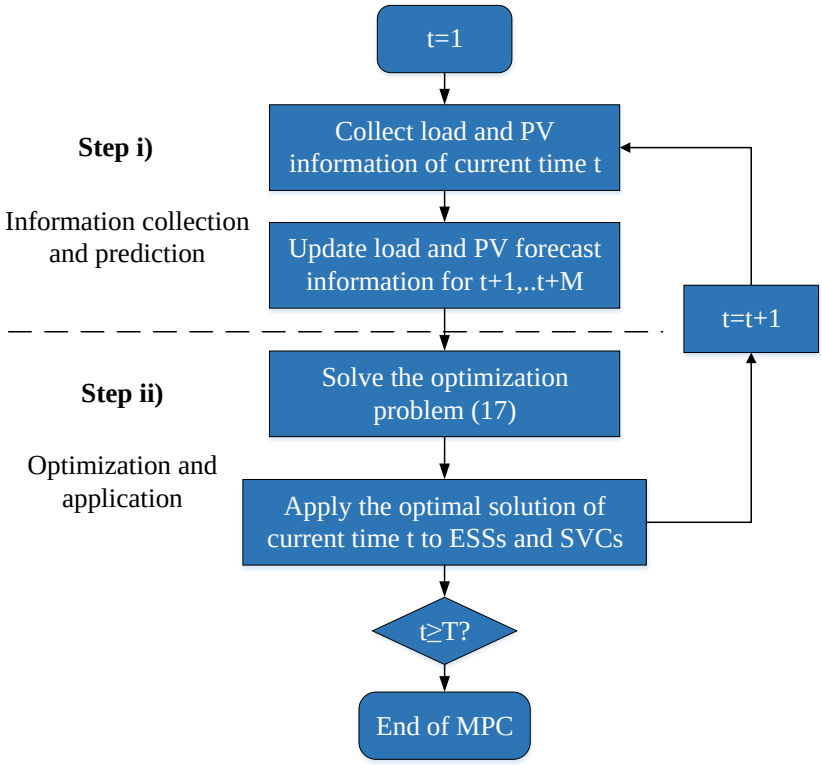

Fig. 4. Flowchart for implementation of the proposed ramp minimization model

4 Case Studies

In this section, we test our proposed MPC based dispatch model, denoted as **MPC**, on the modified IEEE 37-bus distribution network for the ramp minimization over a day. Detailed information of the network can be found in [26]. The nominal voltage value of the distribution system is 4.8kV and per-unit value is used in the case studies. Fig. 5 shows the network topology of IEEE 37-bus distribution feeder with 20 distributed PV installations and 10 distributed ESSs. Eight SVCs are integrated at bus 5, 9, 10, 20, 23, 26, 29 and 34, respectively. Fig. 6 depicts the realized total active load and PV generation of the considered day and the detailed data is provided in Table IV in the Appendix. The parameters related to the PV system, ESS and SVC are listed in Table I along with other parameters.

Table I: Parameters for MPC based dispatch model

PV system capacity $p_j^{g,\max}$	200 kW	Unit degradation cost c_j^d	\$10/MWh
Maximum charging power $p_j^{c,\max}$	200 kW	SVC capacity	200 kVar
Maximum discharging power $p_j^{d,\max}$	200 kW	Lower voltage limit $V_j^{\min}$	0.95 p.u.
Minimum allowed SOC level $S_j^{\min}$	100 kWh	Upper voltage limit $V_j^{\max}$	1.05 p.u.
Maximum allowed SOV level $S_j^{\max}$	1000 kWh	Ramping price c_τ^r	\$50/MW
Charging efficiency η_j^c	95%	Electricity price c_τ^e	\$50/MWh
Discharging efficiency η_j^d	95%		

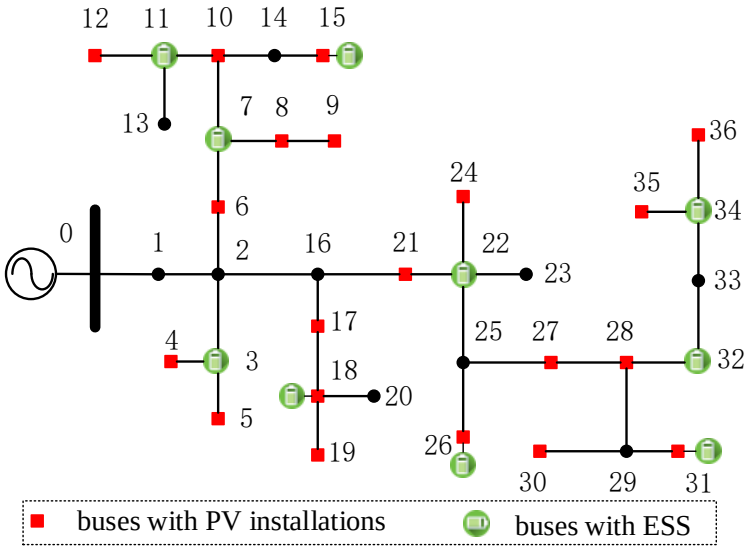

Fig. 5. IEEE 37-bus distribution network with PV installations and ESS

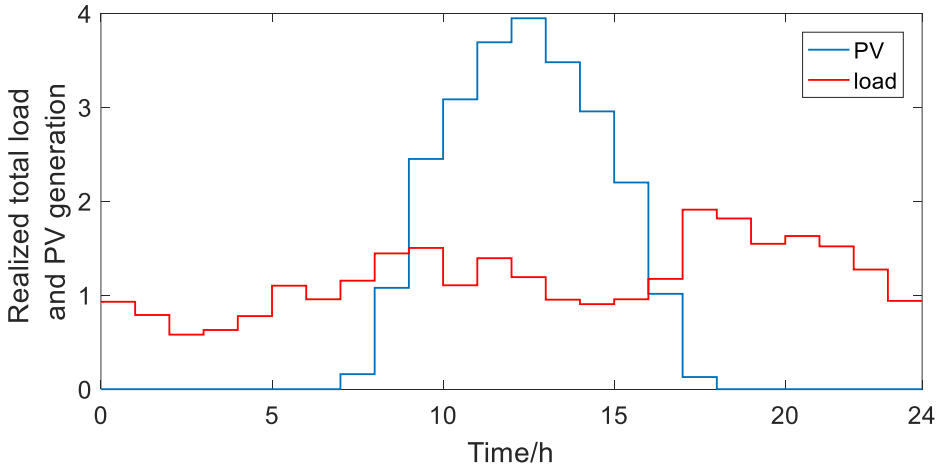

Fig. 6. Realized total active load and PV generation of the distribution network

4.1 Performance Comparisons

1) Comparison with Two Benchmarks

To better justify our proposed ramp minimization method, two benchmarks are used for comparison. Specifically, the first benchmark [11], denoted as **BM1**, aims at flattening the daily net load profile of a distribution network using distributed ESSs. Its mathematical formulation is given as

$$\begin{aligned} \min_{p^c_{m,t},\, p^d_{m,t},\, K,\, \theta} \quad & K \\ \text{s.t} \quad & \left| p_{0,t} - \theta \right| \le K \qquad \forall t \\ & \text{(17b)-(17g)} \qquad \forall t \end{aligned} \tag{BM1}$$

where θ is the target value when the load profile is entirely flattened and K denotes the largest deviation of the load profile to the target value. The second benchmark [12], denoted as **BM2**, utilizes ESSs to minimize the daily operation cost of a distribution network, which is composed of the energy purchase cost from the main grid and ESS degradation cost. Note that in [12], the operation cost also includes dispatch DG operation cost, but it is included in this case since no dispatch DG is considered. The optimization model of BM2 is given as follows,

$$\begin{aligned} \min_{p^c_{j,t},\, p^d_{j,t}} \quad & \sum_{t \in T} \left(c^p_t\, p_{0,t} + \sum_{k \in \mathcal{N}^{ess}} C^d_{k,t} \right) \\ \text{s.t.} \quad & \text{(17b)-(17g)} \qquad \forall t \end{aligned} \tag{BM2}$$

where c^p_t denotes the electricity price at time t, and $C^d_{k,t}$ is the degradation cost of k-th ESS at time t. The time-of-use rate (TOU) in Ontario retail market [27] is used to represent electricity price, as shown by Table II. The periods are customized to accommodate high PV penetration. Note that both benchmarks are solved day-ahead with predicted load demand and PV output. The actual load demand and PV output are random variables and

assumed to be varying within the interval between 70% and 130% of the predicted values.

Table II: Customized time-of-use rate in the case studies

	Period	Price $ per kWh
Off-peak	00:00-9:00	$0.065
Mid-peak	9:00-16:00	$0.094
On-peak	17:00-24:00	$0.132

Fig. 7 shows the daily net load profiles of the distribution system under different cases. The net load without ESS integration is also depicted for comparison. We can see from the figure that all three methods make great contribution to the peak shaving and valley filling. It is straightforward to understand how both benchmarks bring about this effect since the objective of BM1 is to flatten the net load profile and the TOU rate in BM2 is designed to encourage the load shifting from the peak load periods to the valley load periods. Although the goal of our model is to mitigate the ramping effect, it also contributes to the peak shaving and valley filling. The reason is that by minimizing the ramp index between any two successive time slots, the distance between the peak load and valley load is minimized as well. We can also observe from the figure that without ESS, the net load experiences a severe ramp-down event from 8:00 to 10:00 and a severe ramp-up event from 16:00 to 17:00 due to the rapid variation of PV output. It is expected that ESS can substantially mitigate the ramping effect. However, different approaches perform differently on the ramp mitigation. To further illustrate this point, we depict the daily ramp index profile under different cases in Fig. 8. It can be seen that BM1 only slightly reduces the ramp indices. The reason is that it only focuses on minimizing the load variance between the peak load and valley load without considering the load variance between successive time slots. BM2 has a better performance in terms of ramp mitigation compared with BM1, but some ramps in BM2 are still considerably large, such as those at 10:00 and

17:00. However, the ramps are maintained at a low level over the whole day using our proposed method, as shown by the curve denoted as MPC.

Fig. 9 demonstrates the maximum ramp under different cases. We can see that BM1 only reduces the maximum ramp by 30%, while BM2 and our method reduce that by 50% and 74%, respectively. Moreover, the maximum ramp using our method is almost as half as that in BM2. Therefore, our proposed method outperforms both benchmarks in terms of ramp minimization.

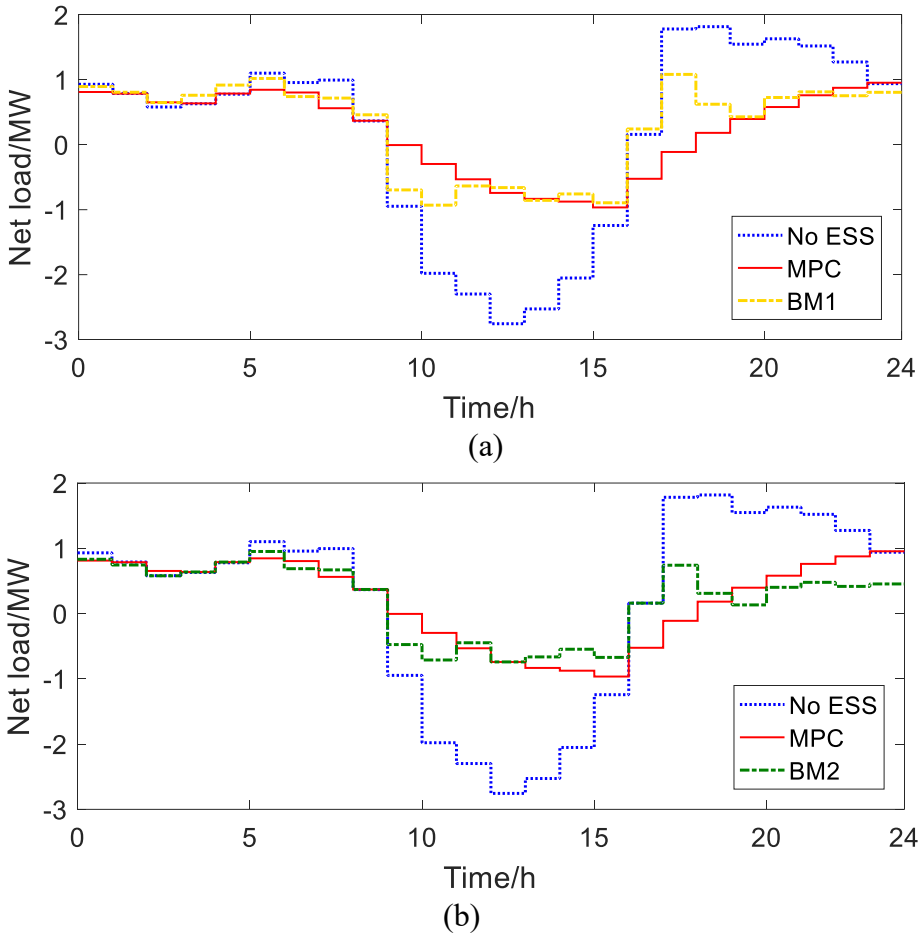

Fig. 7. Daily net load profiles of the distribution system under different cases, (a) comparison between MPC and BM1, (b) comparison between MPC and BM2

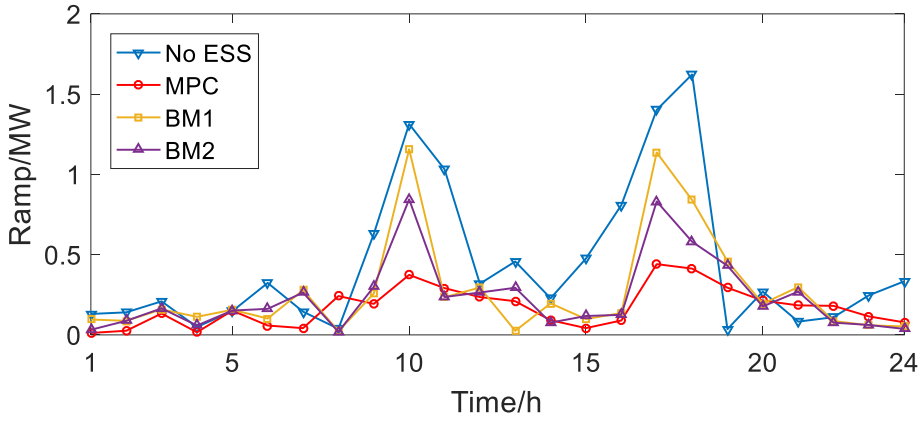

Fig. 8. Daily ramp index profile of the distribution system under different cases

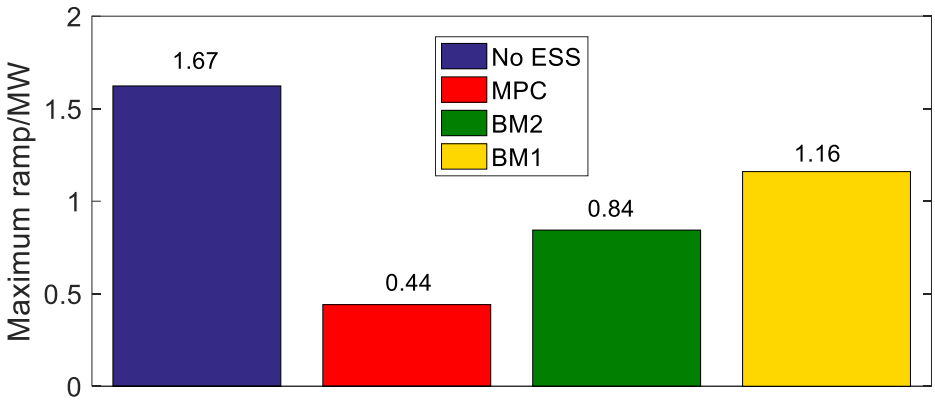

Fig. 9. Maximum ramp index under different cases

To verify our proposed method is also economically efficient, we list the energy purchase cost, ESS degradation cost and the total operation cost of the three cases in Table III. We can observe that BM2 has the lowest total cost as expected. But the total cost in our case is just slightly higher (about 0.6%) than that in BM2. Therefore, our proposed MPC based ramp minimization model is economically efficient.

Table III: Cost comparison using different methods

	BM1	BM2	MPC
Energy purchase Cost ($)	1026	720	725
ESS Degradation cost ($)	148	180	180
Total cost ($)	1174	900	905

2) Comparison with Single-period Model

To verify the superiority of the MPC method, we compare the results of our case with the result using single-period ramp minimization model, denoted as **Single-t.** Each time only one time slot is considered in the Single-t model. Fig. 11 plots the daily ramp index profile under MPC and Single-t. It can be observed that the ramp mitigation performance under MPC is much better than that under Single-t. The maximum ramp index is only reduced by 18.5% under Single-t. In contrast, it is reduced by 74% under MPC. The reason is that MPC based model takes future forecast information into account and thus allocates the ESS charging and discharging power more appropriately to deal with the forthcoming ramp event. Fig. 11 shows the total charging/discharging power under MPC and Single-t. We can see that the charging/discharging power under Single-t is larger than that under MPC at the beginning of the ramp event. Thus, the charging/discharging power under Single-t cannot last for a long period due to the limit of ESS capacity. Consequently, the ramp mitigation capability of ESSs is greatly impaired.

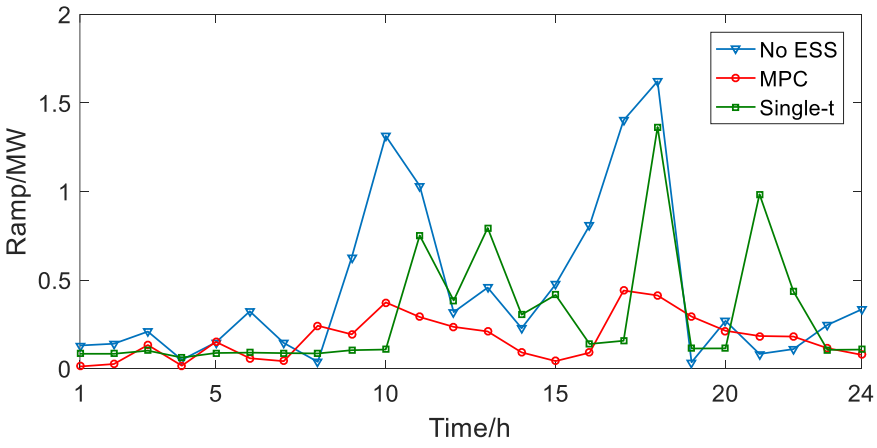

Fig. 10. Daily ramp indices under MPC and single t

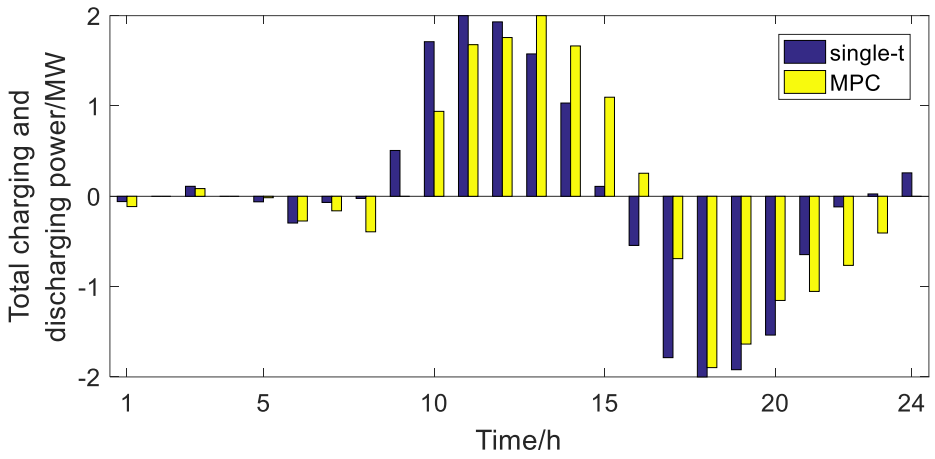

Fig. 11. Total charging (-) and discharging (+) power of ESSs under MPC and single t

4.2 Sensitivity Analysis

In this subsection, we conduct a sensitivity analysis of the maximum ramp and total operation cost to the ESS capacity. We denote the ESS capacity and power rating used in the last subsection as the unit one (100%). Each time we reduce the ESS capacity and power rating by 10% and run the simulations with the same other parameters. Fig. 12 illustrates the relationship between the maximum ramp and ESS capacity. It can be seen that the maximum ramp almost decreases linearly with the increase of ESS capacity, which implies the ramp mitigation capability depends linearly on the ESS capacity within the considered range. Fig. 13 shows the relationship between the ESS capacity and the total operation cost. We can see that the total operation cost declines linearly with the growth of ESS capacity. Hence, the ESS capacity has a great impact on the reduction of maximum ramp and the total operation cost. However, the expansion of ESS capacity results in considerably high investment cost. Thus, there is a trade-off between saving investment cost and improving the ramp mitigation capability via ESS expansion.

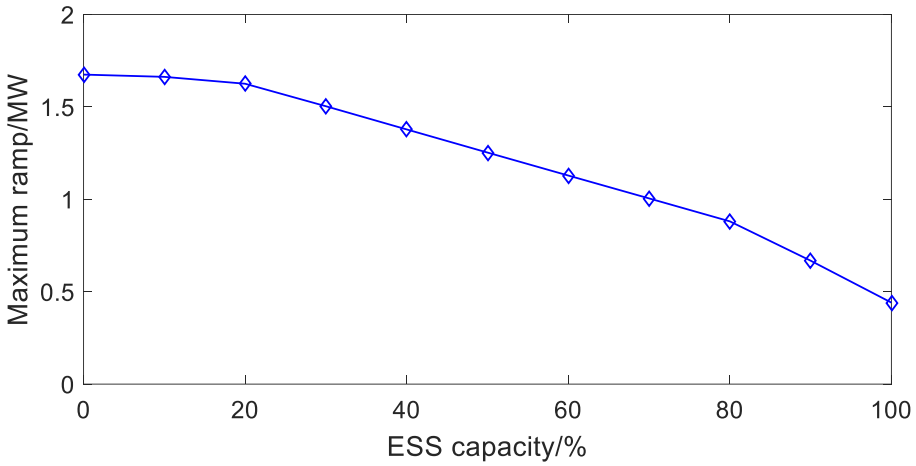

Fig. 12. Maximum ramp under different ESS capacities

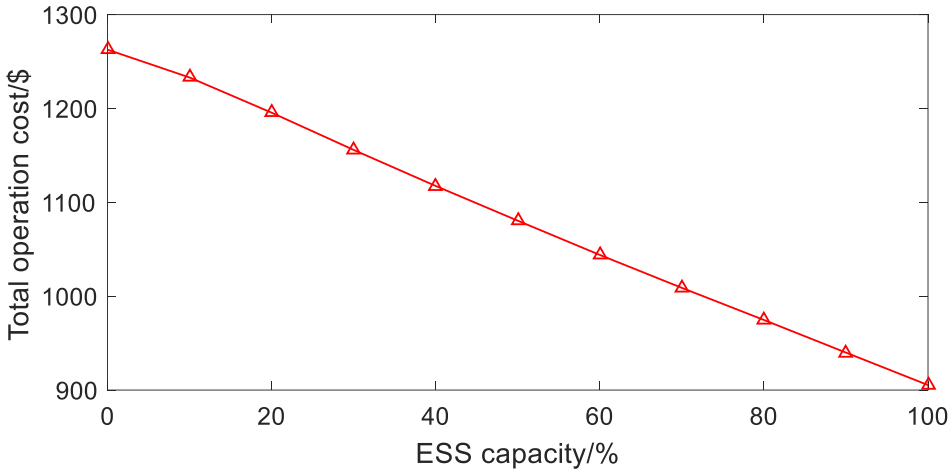

Fig. 13. Total cost under different ESS capacities

5 Conclusions

The distribution networks are under a transition from passive ones to active ones with the increasing integration of distributed generations. However, the significant variation of renewable energy generations, especially the rooftop PV systems, will aggravate the ramp-events in transmission networks. Aiming to address this issue, we propose a novel MPC based dispatch model to minimize ramping effect in active DNs using distributed ESSs. In particular, we model the dispatch model with ESS scheduling as a multi-period optimization problem which is carried out using the MPC method. Since the MPC method

considers both current and future information, it will produce an appropriate ESS scheduling result and keep the ramp at low level over the whole day. Moreover, second-order cone relaxed branch flow model is used to model the power flow in DNs so as to guarantee the global optimality. Case study on IEEE 37-bus distribution network demonstrates that our proposed model brings about significant reduction of maximum ramp and yields economically efficient results.

Acknowledgement

This work was partially supported by Research Grants Council of Hong Kong, China under Grant No. T23-407/13N and T23-701/14N.

Appendix

Table IV: Total load and PV of the considered day

Hour	Load/MW	PV/MW	Hour	Load/MW	PV/MW	Hour	Load/MW	PV/MW
1	0.93	0	9	1.45	1.08	17	1.17	1.02
2	0.79	0	10	1.50	2.45	18	1.91	0.13
3	0.58	0	11	1.11	3.09	19	1.82	0
4	0.63	0	12	1.39	3.69	20	1.55	0
5	0.78	0	13	1.19	3.95	21	1.63	0
6	1.10	0	14	0.95	3.48	22	1.52	0
7	0.96	0	15	0.91	2.96	23	1.27	0
8	1.16	0.16	16	0.96	2.20	24	0.94	0

Reference

[1] J. Zhao, J. Wang, Z. Xu, C. Wang, C. Wan, and C. Chen, "Distribution Network Electric Vehicle Hosting Capacity Maximization: A Chargeable Region Optimization Model," *IEEE Transactions on Power Systems,* vol. 32, pp. 4119-4130, 2017.

[2] J. Zhang, H. Cheng, and C. Wang, "Technical and economic impacts of active management on distribution network," *International Journal of Electrical Power & Energy Systems,* vol. 31, pp. 130-138, 2009.

[3] M. Ahlstrom, E. Ela, J. Riesz, J. O. Sullivan, B. F. Hobbs, M. O. Malley*, et al.*, "The Evolution of the Market: Designing a Market for High Levels of Variable Generation," *IEEE Power and Energy Magazine,* vol. 13, pp. 60-66, 2015.

[4] C. Wu, G. Hug, and S. Kar, "Risk-Limiting Economic Dispatch for Electricity Markets With Flexible Ramping Products," *IEEE Transactions on Power Systems,* vol. 31, pp. 1990-2003, 2016.

[5] P. Denholm, M. O'Connell, G. Brinkman, and J. Jorgenson, "Overgeneration from Solar Energy in California. A Field Guide to the Duck Chart," National Renewable Energy Lab.(NREL), Golden, CO (United States)2015.

[6] B. I. Crăciun, T. Kerekes, D. Séra, R. Teodorescu, and U. D. Annakkage, "Power Ramp Limitation Capabilities of Large PV Power Plants With Active Power Reserves," *IEEE Transactions on Sustainable Energy,* vol. 8, pp. 573-581, 2017.

[7] L. Xu and D. Tretheway, "Flexible Ramping Products," 2012.

[8] Q. Wang and B. M. Hodge, "Enhancing Power System Operational Flexibility With Flexible Ramping Products: A Review," *IEEE Transactions on Industrial Informatics,* vol. 13, pp. 1652-1664, 2017.

[9] Y. Zhang, V. Gevorgian, C. Wang, X. Lei, E. Chou, R. Yang*, et al.*, "Grid-Level Application of Electrical Energy Storage: Example Use Cases in the United States and China," *IEEE Power and Energy Magazine,* vol. 15, pp. 51-58, 2017.

[10] H. Khani, M. R. D. Zadeh, and A. H. Hajimiragha, "Transmission Congestion Relief Using Privately Owned Large-Scale Energy Storage Systems in a Competitive Electricity Market," *IEEE Transactions on Power Systems,* vol. 31, pp. 1449-1458, 2016.

[11] Y. Zhang, A. Melin, M. Olama, S. Djouadi, J. Dong, and K. Tomsovic, "Battery energy storage scheduling for optimal load variance minimization," in *2018 IEEE Power & Energy Society Innovative Smart Grid Technologies Conference (ISGT)*, 2018, pp. 1-5.

[12] L. H. Macedo, J. F. Franco, M. J. Rider, and R. Romero, "Optimal Operation of Distribution Networks Considering Energy Storage Devices," *IEEE Transactions on Smart Grid,* vol. 6, pp. 2825-2836, 2015.

[13] C. O. Dwyer and D. Flynn, "Using Energy Storage to Manage High Net Load Variability at Sub-Hourly Time-Scales," *IEEE Transactions on Power Systems,* vol. 30, pp. 2139-2148, 2015.

[14] Y. Wen, C. Guo, H. Pandzic, and D. S. Kirschen, "Enhanced Security-Constrained Unit Commitment With Emerging Utility-Scale Energy Storage," *Power Systems, IEEE Transactions on,* vol. PP, pp. 1-11, 2015.

[15] A. Bhattacharya, J. Kharoufeh, and B. Zeng, "Managing Energy Storage in Microgrids: A Multistage Stochastic Programming Approach," *IEEE Transactions*

on Smart Grid, vol. PP, pp. 1-1, 2016.
[16] J. Li, Z. Xu, J. Zhao, and C. Wan, "A Coordinated Dispatch Model for Distribution Network Considering PV Ramp," *IEEE Transactions on Power Systems,* vol. PP, pp. 1-1, 2017.
[17] C. Chen, J. Wang, Y. Heo, and S. Kishore, "MPC-Based Appliance Scheduling for Residential Building Energy Management Controller," *IEEE Transactions on Smart Grid,* vol. 4, pp. 1401-1410, 2013.
[18] D. E. Olivares, C. A. Canizares, and M. Kazerani, "A Centralized Energy Management System for Isolated Microgrids," *IEEE Transactions on Smart Grid,* vol. 5, pp. 1864-1875, 2014.
[19] L. Jin, R. Kumar, and N. Elia, "Model Predictive Control-Based Real-Time Power System Protection Schemes," *IEEE Transactions on Power Systems,* vol. 25, pp. 988-998, 2010.
[20] M. E. Baran and F. F. Wu, "Optimal capacitor placement on radial distribution systems," *IEEE Transactions on Power Delivery,* vol. 4, pp. 725-734, 1989.
[21] M. Baran and F. F. Wu, "Optimal sizing of capacitors placed on a radial distribution system," *IEEE Transactions on Power Delivery,* vol. 4, pp. 735-743, 1989.
[22] M. Farivar and S. H. Low, "Branch Flow Model: Relaxations and Convexification--Part I," *IEEE Transactions on Power Systems,* vol. 28, pp. 2554-2564, 2013.
[23] D. T. Nguyen and L. B. Le, "Optimal Bidding Strategy for Microgrids Considering Renewable Energy and Building Thermal Dynamics," *IEEE Transactions on Smart Grid,* vol. 5, pp. 1608-1620, 2014.
[24] C. Wan, J. Lin, Y. Song, Z. Xu, and G. Yang, "Probabilistic Forecasting of Photovoltaic Generation: An Efficient Statistical Approach," *IEEE Transactions on Power Systems,* vol. 32, pp. 2471-2472, 2017.
[25] S. Chai, Z. Xu, and W. K. Wong, "Optimal Granule-Based PIs Construction for Solar Irradiance Forecast," *IEEE Transactions on Power Systems,* vol. 31, pp. 3332-3333, 2016.
[26] D. T. F. W. Group, "Distribution test feeders," *Available from: ewh. ieee. org/soc/pes/dsacom/testfeeders/index. htmi,* 2010.
[27] "Time-of-use rate in Ontario," [Online]. Available: http://www.ieso.ca/power-data/price-overview/time-of-use-rates.